



CrossMark  
click for updates

Cite this: *RSC Adv.*, 2016, 6, 43470

# Electrochemically fabricated electrochromic films from 4-(*N*-carbazolyl)triphenylamine and its dimethoxy derivative†

Sheng-Huei Hsiao\* and Hui-Min Wang

A carbazolyl-substituted triphenylamine derivative, 4-(*N*-carbazolyl)triphenylamine (TPACz), was synthesized and used to build a fluorescent and electrochromic polymeric film (PTPACz) on the ITO-glass surface by electrochemical oxidative coupling reactions. The electrodeposited PTPACz film showed blue emission ( $\lambda_{\text{max}} = 424 \text{ nm}$ ) and exhibited reversible electrochemical redox processes and stable color changes upon electro-oxidation, which can be switched by potential modulation. The remarkable electrochromic behavior of the film is clearly interpreted on the basis of spectroelectrochemical studies. A dimethoxy-substituted derivative of TPACz, namely 4,4'-dimethoxy-4''-(*N*-carbazolyl)triphenylamine (MeOTPACz), was also synthesized and characterized for a comparative study. Repetitive cyclic voltammetry scanning of MeOTPACz in an electrolyte/acetonitrile solution resulted in an electroactive dimeric film of (MeOTPACz)<sub>2</sub> on the electrode surface. Electrochromic devices using PTPACz or (MeOTPACz)<sub>2</sub> as an active layer were also fabricated as preliminary investigations for electrochromic applications.

Received 3rd April 2016  
Accepted 28th April 2016

DOI: 10.1039/c6ra08528h

www.rsc.org/advances

## Introduction

Electrochromism is the phenomenon displayed by an electroactive species that changes color reversibly in response to an applied electrical charge.<sup>1</sup> A vast number of electrochromic materials have been studied, and transition metal oxides,<sup>2</sup> molecular dyes,<sup>3</sup> and  $\pi$ -conjugated polymers<sup>4</sup> are the most frequently investigated components. Some organic-inorganic coordination polymers have also received great interest for electrochromic applications.<sup>5</sup> In general,  $\pi$ -conjugated polymers show several advantages over the other types of electrochromics, such as high coloration efficiency, rapid switching speeds, high optical contrasts, ease of processing, and the possibility to tune the properties through chemical modification.<sup>6</sup> Potential applications of electrochromic materials include optical switching devices, electrochromic displays, sunglasses, antiglare rear-view mirrors, smart windows for cars or buildings, data storage, electronic papers and adaptive camouflage.<sup>7</sup> Recent high-profile commercialization of electrochromics includes the Boeing 787 Dreamliner windows manufactured by Gentex.<sup>8</sup>

Carbazole and triarylamine derivatives and polymers are well-known for their electroactive and photoactive properties that may find optoelectronic applications in electrophotography, electroluminescent diodes, field-effect transistors, solar cells, memory devices, and electrochromic or electrofluorochromic devices.<sup>9–14</sup>

During the past decade, Liou's group has carried out extensive studies on the design and synthesis of triarylamine-based high-performance polymers such as aromatic polyamides and polyimides for potential electrochromic and memory applications.<sup>15,16</sup> In general, these polymers exhibit good solubility to organic solvents due to the introduction of bulky, packing-disruptive triarylamine moieties. Therefore, the polymeric layers used in the devices can be easily prepared by simple spin-coating or drop-casting methods. As a class of excellent electrochromic and memory materials, these polymers have various useful properties such as easily forming relatively stable polarons (radical cations), high carrier mobility, high thermal stability, and good mechanical properties. Recently, we have reported that aromatic polyamides and polyimides containing 4-(*N*-carbazolyl)triphenylamine (TPACz) segments show attractive electrochemical and electrochromic properties, and incorporating sterically hindered *tert*-butyl or electron-donating methoxy groups at the electrochemically active C-3 and C-6 sites of the carbazole unit leads to a greatly enhanced redox and electrochromic stability of the polymers upon electro-oxidation.<sup>17</sup> In addition to visible absorption, the polarons of these TPACz-based polymers also show strong absorption in near-infrared (NIR) region due to the intervalence-charge transfer (IV-CT) between the TPA and carbazole redox centers.<sup>18,19</sup> Thus, the reported TPACz-containing polymers could be candidates for the applications in organic visible/NIR electrochromic devices.

As reported in the pioneering works by Nelson and Adams *et al.*, unsubstituted triphenylamine (TPA) undergoes dimerization (coupling) to tetraphenylbenzidine (TPB) after the formation of an unstable monocation radical.<sup>20</sup> This is accompanied by the

Department of Chemical Engineering and Biotechnology, National Taipei University of Technology, Taipei 10608, Taiwan. E-mail: shhsiao@ntut.edu.tw

† Electronic supplementary information (ESI) available. See DOI: 10.1039/c6ra08528h

loss of two protons per dimer and the dimer is more easily oxidized than TPA and also can undergo further oxidations in two discrete one-electron steps to give  $\text{TPB}^{2+}$  monocation and finally the quinoidal  $\text{TPB}^{2+}$ . Quantitative data have been obtained for several 4-substituted TPAs in the form of second-order coupling rate constants, and it was generally found that electron-donating substituents such as methoxy group tended to stabilize the cation radicals while the electron-withdrawing groups like nitro group had the opposite effect. On the other hand, the electrochemical oxidation of carbazole and *N*-substituted derivatives was first studied by Ambrose and Nelson.<sup>21a</sup> They further studied systematically 76 ring-substituted carbazoles about their substituent effects using electrochemical and spectroscopic techniques.<sup>21b</sup> For the *N*-phenylcarbazoles (NPCs) with both the 3 and 6 carbazole ring positions unprotected, these compounds underwent an initial one-electron oxidation to generate a very reactive cation radical; two of these then coupled at the 3 positions to yield a *N,N'*-diphenyl-3,3'-bicarbazyl. This species is then oxidized more easily than the corresponding carbazole to a stable dication. The basic difference between TPAs and NPCs is that the carbazoles are planar across two benzene rings while the TPAs have all three rings at angles to each other. Due to the planarity of the carbazole system and the attendant high electron density at the reactive sites, the coupling rate of NPCs has been found to be much faster than for the TPAs. The TPA or carbazole electrochemically oxidative dimerization reaction has been employed efficiently to fabricate electroactive polymer films with potential applications in electronic and optoelectronic devices.<sup>22</sup>

Electrochromic devices have been extensively prepared using solution processable electroactive polymers.<sup>23</sup> This is in part because accurate assessment of optical and electrochemical polymer properties rely on solution based techniques. Electrochromic devices also could be assembled using electrochromic polymers electro-deposited on ITO glass electrodes.<sup>24</sup> Electrochemical polymerization provides the unique advantage to combine both synthesis and direct fabrication of electroactive polymer films on the electrode surface. This procedure significantly shortens the experimental time and avoids the solubility issues often encountered with conventional chemical methods, thus enlarging the scope of candidate polymers for electrochromic applications. As a continuation of our recent efforts in developing electrochromic materials by electrochemical synthesis, herein we study the electrochemical polymerization of a novel simple monomer **TPACz** and the electrochemical, electro-optical, and electrochromic properties of its electro-deposited polymer films (**PTPACz**) on ITO-glass substrate. For a comparative study, an analogous derivative **MeOTPACz** with methoxy groups substituted on the active sites of the TPA unit was also synthesized, and its electrochemical behavior was investigated. Oxidative coupling reactions between **MeOTPACz** molecules only produced a dimer (**MeOTPACz**)<sub>2</sub>. This work provides a model to design **TPACz** derivatives capable to form electrochemically active polymers with potential applications in electronic and optoelectronic devices. Single layer electrochromic devices based on **PTPACz** and (**MeOTPACz**)<sub>2</sub> are also constructed and characterized. These devices show good electrochromic stability and high optical contrast ratios.

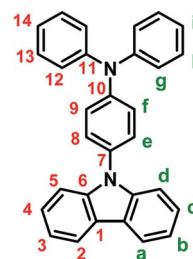
## Experimental

### Materials

According to the reported procedure,<sup>15b</sup> *N*-(4-aminophenyl) carbazole was prepared by the cesium fluoride-mediated aromatic nucleophilic substitution reaction of 4-fluoronitrobenzene with carbazole followed by Pd/C-catalyzed hydrazine reduction in refluxing ethanol. Iodobenzene (TCI), 4-iodoanisole (ACROS), copper powder (ACROS), potassium carbonate ( $\text{K}_2\text{CO}_3$ , SHOWA), triethylene glycol dimethyl ether (TEGDME, ACROS), iron(III) chloride (ACROS), nitrobenzene (ACROS), chloroform (TEDIA) and tetrahydrofuran (THF, TEDIA) were used without further purification. All electrochemical and spectroelectrochemical studies were performed using acetonitrile (ACN, Tedia) solutions containing tetrabutylammonium perchlorate (TBAP, TCI) as the supporting electrolyte. TBAP was recrystallized twice from ethyl acetate under nitrogen atmosphere and then dried *in vacuo* before use. Acetonitrile was dried over calcium hydride for 24 h, distilled under reduced pressure, and stored over 4 Å molecular sieves in a sealed bottle. All other reagents were used as received from commercial sources.

### Monomer synthesis

**4-(*N*-Carbazolyl)triphenylamine (TPACz)**. A mixture of *N*-(4-aminophenyl)carbazole (8.5 g, 33 mmol), iodobenzene (16.3 g, 80 mmol), copper powder (5.1 g, 80 mmol), potassium carbonate (22.1 g, 160 mmol), and TEGDME (30 mL) was stirred under nitrogen atmosphere at 180 °C for 24 h. The brown precipitate was collected by filtration and washed thoroughly by water. The crude product was filtered and recrystallized from acetonitrile to afford 8.3 g (61% in yield) of brown crystals with an mp of 172–174 °C (by DSC at a heating rate of 2 °C min<sup>-1</sup>). <sup>1</sup>H NMR (500 MHz,  $\text{CDCl}_3$ ,  $\delta$ , ppm): 7.14 (t,  $J = 7.5$  Hz, 2H, H<sub>i</sub>), 7.27 (d,  $J = 7.5$  Hz, 4H, H<sub>g</sub>), 7.31 (d,  $J = 8.8$  Hz, 2H, H<sub>f</sub>), 7.33 (t,  $J = 7.5$  Hz, 2H, H<sub>b</sub>), 7.37 (t,  $J = 7.5$  Hz, 4H, H<sub>h</sub>), 7.44 (d,  $J = 9.5$  Hz, 2H, H<sub>e</sub>), 7.47 (t,  $J = 7.5$  Hz, 2H, H<sub>c</sub>), 7.50 (d,  $J = 7.5$  Hz, 2H, H<sub>d</sub>). <sup>13</sup>C NMR (125 MHz,  $\text{CDCl}_3$ ,  $\delta$ , ppm): 109.8 (C<sup>5</sup>), 119.7 (C<sup>3</sup>), 120.2 (C<sup>2</sup>), 123.2 (C<sup>1</sup>), 123.5 (C<sup>14</sup>), 124.0 (C<sup>9</sup>), 124.7 (C<sup>12</sup>), 125.8 (C<sup>4</sup>), 127.8 (C<sup>8</sup>), 129.4 (C<sup>13</sup>), 131.4 (C<sup>7</sup>), 141.1 (C<sup>6</sup>), 147.1 (C<sup>10</sup>), 147.5 (C<sup>11</sup>). Crystal data: pale brown crystal grown during the slow crystallization in acetonitrile, 0.40 × 0.34 × 0.14 mm, monoclinic *C2/c* with  $a = 27.8714(16)$ ,  $b = 9.7479(5)$ ,  $c = 19.7603(9)$  Å;  $\alpha = 90^\circ$ ,  $\beta = 126.516(3)^\circ$ ,  $\gamma = 90^\circ$ , where density of crystal  $D_c = 1.264$  Mg m<sup>-3</sup> for  $Z = 8$  and  $V = 4314.7(4)$  Å<sup>3</sup>. The molecular structure of **TPACz** by single crystal X-ray analysis is shown in Fig. 1.



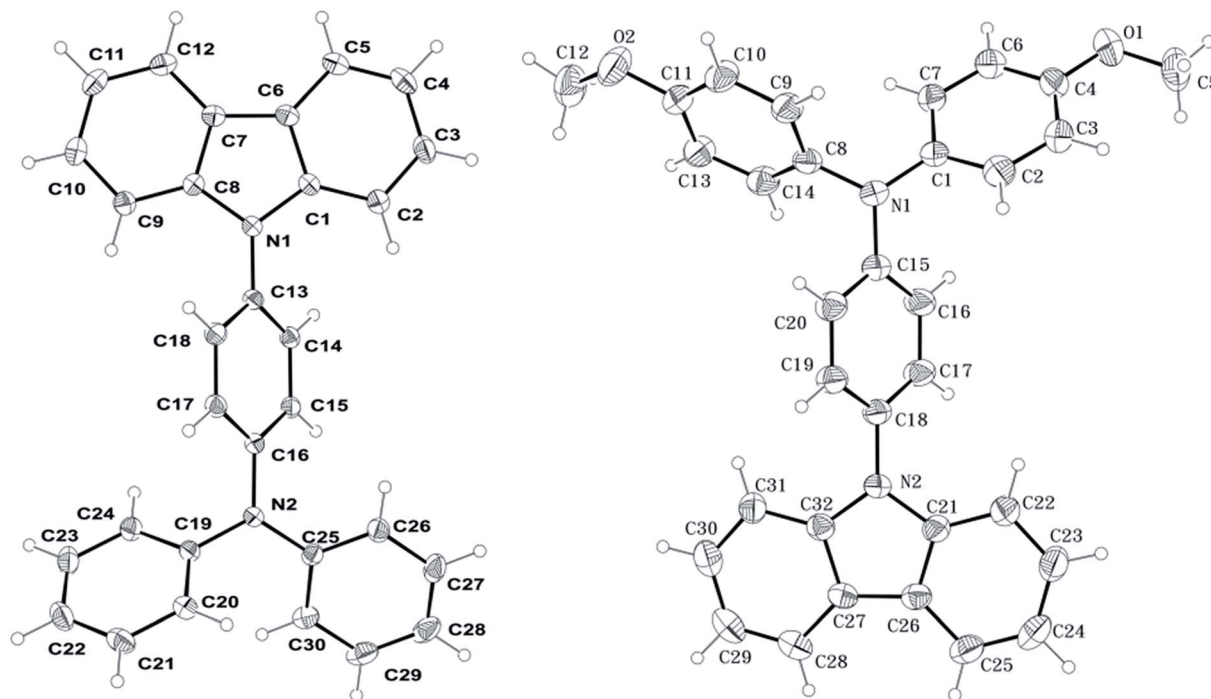
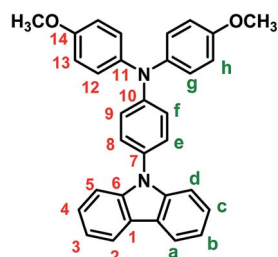


Fig. 1 Molecular structures of TPACz and MeOTPACz by single crystal X-ray analysis.

**4,4'-Dimethoxy-4''-(*N*-carbazolyl)triphenylamine (MeOTPACz).** A mixture of *N*-(4-aminophenyl)carbazole (8.5 g, 33 mmol), 4-iodoanisole (18.7 g, 80 mmol), copper powder (5.1 g, 80 mmol), potassium carbonate (22.1 g, 160 mmol), and TEGDME (30 mL) was stirred under nitrogen atmosphere at 180 °C for 24 h. The brown precipitate was collected by filtration and washed thoroughly by water. The crude product was filtered and recrystallized from acetonitrile to afford 8.5 g (55% in yield) of brown crystals with an mp of 126–127 °C (by DSC at a heating rate of 2 °C min<sup>-1</sup>). <sup>1</sup>H NMR (500 MHz, CDCl<sub>3</sub>, δ, ppm): 3.84 (s, 6H, -OCH<sub>3</sub>), 6.92 (d, *J* = 8.8 Hz, 4H, H<sub>h</sub>), 7.12 (d, *J* = 8.7 Hz, 2H, H<sub>f</sub>), 7.20 (d, *J* = 8.8 Hz, 4H, H<sub>g</sub>), 7.30 (m, 2H, H<sub>b</sub>), 7.33 (d, *J* = 8.7 Hz, 2H, H<sub>e</sub>), 7.43 (m, 4H, H<sub>c</sub> + H<sub>d</sub>), 8.16 (d, *J* = 7.7 Hz, 2H, H<sub>a</sub>). <sup>13</sup>C NMR (125 MHz, CDCl<sub>3</sub>, δ, ppm): 55.49 (-OCH<sub>3</sub>), 109.84 (C<sup>5</sup>), 114.87 (C<sup>13</sup>), 119.53 (C<sup>3</sup>), 120.19 (C<sup>2</sup>), 120.58 (C<sup>9</sup>), 123.08 (C<sup>1</sup>), 125.74 (C<sup>4</sup>), 126.96 (C<sup>12</sup>), 127.72 (C<sup>8</sup>), 129.39 (C<sup>7</sup>), 140.62 (C<sup>11</sup>), 141.26 (C<sup>6</sup>), 148.14 (C<sup>10</sup>), 156.22 (C<sup>14</sup>). Crystal data: pale brown crystal grown during the slow crystallization in acetonitrile, 0.44 × 0.24 × 0.14 mm, monoclinic *C*2/*c* with *a* = 9.2535(2), *b* = 13.8327(3), *c* = 19.4070(5) Å; α = 90°, β = 90°, γ = 90°, where density of crystal *D*<sub>c</sub> = 1.258 Mg m<sup>-3</sup> for *Z* = 4 and *V* = 2484.03(10) Å<sup>3</sup>. The molecular structure of MeOTPACz by single crystal X-ray analysis is shown in Fig. 1.



### Electrochemical polymerization/dimerization

Electrochemical polymerization or dimerization was performed with a CH Instruments 750A electrochemical analyzer. The polymers were synthesized from  $1.0 \times 10^{-3}$  M TPACz or MeOTPACz in 0.1 M TBAP/ACN solution *via* cyclic voltammetry repetitive cycling at a scan rate of 150 mV s<sup>-1</sup> during ten cycles. The polymer was deposited onto the surface of the working electrode (platinum disc or ITO/glass surface, polymer films area about 0.8 cm × 1.25 cm), and the film was rinsed with plenty of acetone for the removal of inorganic salts and other organic impurities formed during the process.

### Fabrication of electrochromic devices (ECDs)

The PTPACz polymer and (MeOTPACz)<sub>2</sub> dimer films were electro-deposited on the ITO-coated glass substrate by the electrochemical oxidative coupling method described above. A gel electrolyte based on PMMA (*M*<sub>w</sub>: 120 000) and LiClO<sub>4</sub> was plasticized with propylene carbonate to form a highly transparent and conductive gel. PMMA (1 g) was dissolved in dry ACN (4 mL), and LiClO<sub>4</sub> (0.1 g) was added to the polymer solution as supporting electrolyte. Then propylene carbonate (1.5 g) was added as plasticizer. The mixture was then gently heated until gelation. The gel electrolyte was spread on the polymer-coated side of the electrode, and the electrodes were sandwiched. Finally, an epoxy resin was used to seal the device.

### Instrumentation

Infrared (IR) spectra were recorded on a Horiba FT-720 FT-IR spectrometer. <sup>1</sup>H and <sup>13</sup>C NMR spectra were measured on a Bruker Avance 500 FT-NMR system with tetramethylsilane as

an internal standard. X-ray single crystal diffraction experiment was carried out on a Norius Kappa CCD four-circle diffractometer equipped with graphite-monochromated Mo-K $\alpha$  radiation. The structure was solved by direct methods using SHELXL-97 software. Ultraviolet-visible (UV-vis) spectra of the polymer films were recorded on an Agilent 8453 UV-visible spectrometer. The absorption spectra of monomers and polymers were recorded in CH<sub>2</sub>Cl<sub>2</sub> or as electrodeposited thin films on ITO/glass substrate. The optical band gaps ( $E_g$ ) of monomers and polymers were calculated from their absorption edges. Photoluminescence (PL) spectra were measured with a Varian Cary Eclipse fluorescence spectrophotometer. Fluorescence quantum yields ( $\Phi_F$ ) of the samples in different solvent were measured by using quinine sulfate in 1 N H<sub>2</sub>SO<sub>4</sub> as a reference standard ( $\Phi_F = 54.6\%$ ). Electrochemistry was performed with a CHI 750A electrochemical analyzer. Cyclic voltammetry was conducted with the use of a three-electrode cell in which ITO (polymer films area about 0.8 cm  $\times$  1.25 cm) was used as a working electrode. A platinum wire was used as an auxiliary electrode. All cell potentials were taken with the use of a ALS RE-1B (Ag/AgCl, 3 M NaCl) reference electrode. Ferrocene was used as an external reference for calibration (+0.48 V vs. Ag/AgCl). Spectroelectrochemical experiments were carried out in a cell built from a commercial UV-visible cuvette using an Agilent 8453 UV-visible diode array spectrophotometer. The cell was composed of a 1 cm cuvette, ITO as a working electrode, a platinum wire as an auxiliary electrode, and a Ag/AgCl reference electrode. Photographs of the polymer films were taken by using a Ricoh R7 digital camera.

## Results and discussion

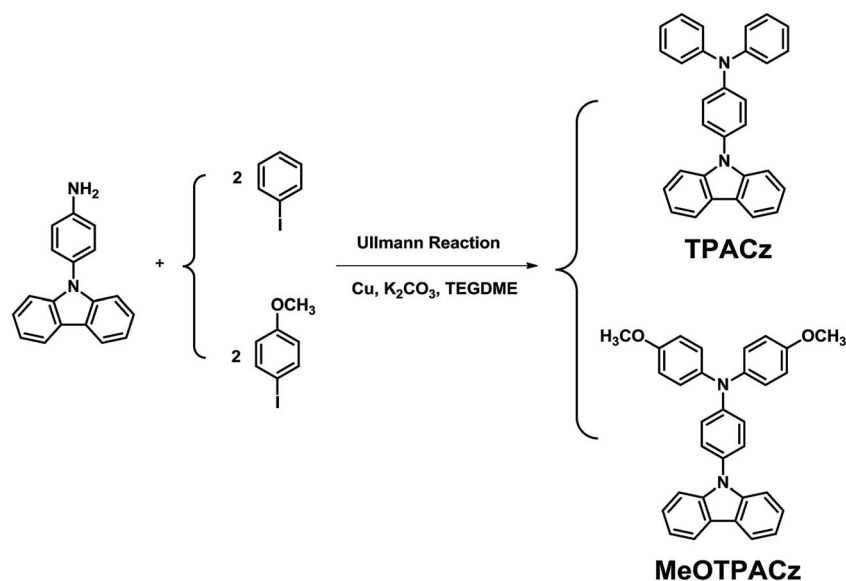
### Monomer synthesis

The synthetic route of monomers is outlined in Scheme 1. **TPACz** and **MeOTPACz** were prepared by Ullmann reaction from

*N*-(4-aminophenyl)carbazole with iodobenzene and 4-iodoanisole, respectively. IR, NMR spectroscopic techniques and X-ray crystal analysis were used to confirm the structures of the obtained monomers. IR spectra of **TPACz** and **MeOTPACz** are included in ESI Fig. S1.† The methoxy groups of **MeOTPACz** present characteristic absorption ( $-\text{OCH}_3$ , sp<sup>3</sup> C–H stretching) in the range 2837–2950 cm<sup>-1</sup>. No absorption bands due to the NH<sub>2</sub> stretching of *N*-(4-aminophenyl)carbazole around 3200–3400 cm<sup>-1</sup> can be observed in Fig. S1.† The <sup>1</sup>H and <sup>13</sup>C NMR spectra of **TPACz** and **MeOTPACz** are illustrated in ESI Fig. S2 and S3,† respectively. Assignments of each proton and carbon were assisted by the two dimensional H–H COSY and C–H HMQC spectra given in ESI Fig. S4 and S5,† and the results agreed well with the proposed molecular structures of **TPACz** and **MeOTPACz**. The molecular structures of **TPACz** and **MeOTPACz** were also confirmed by single-crystal X-ray acquired from the single crystal obtained by slow crystallization of an acetonitrile solution, and the bond length and angle data are summarized in ESI Table S1.† As shown in Fig. 1, **TPACz** and **MeOTPACz** display a coplanar structure of the carbazolyl unit and a propeller-shaped conformation of the triphenylamine core.

### Electrochemical oxidative coupling

The electrochemical oxidative coupling reactions of monomers were carried out on the ITO glass slides in 0.1 M TBAP/ACN solution containing  $1.0 \times 10^{-3}$  M **TPACz** or **MeOTPACz** via repetitive cycling at a potential scan rate of 150 mV s<sup>-1</sup>. Fig. 2(a) displays the successive cyclic voltammograms (CV) of the **TPACz** solution between 0 and 1.8 V. In the first anodic half-cycle, two peaks are observed at  $E_{pa} = 1.07$  and 1.55 V, which are attributed to the oxidation of TPA and carbazole unit, respectively, resulting in formation of oligomers/polymer in the vicinity of electrode surface. In the reverse scan, two peaks are detected at



Scheme 1 Synthetic route to monomers **TPACz** and **MeOTPACz**.

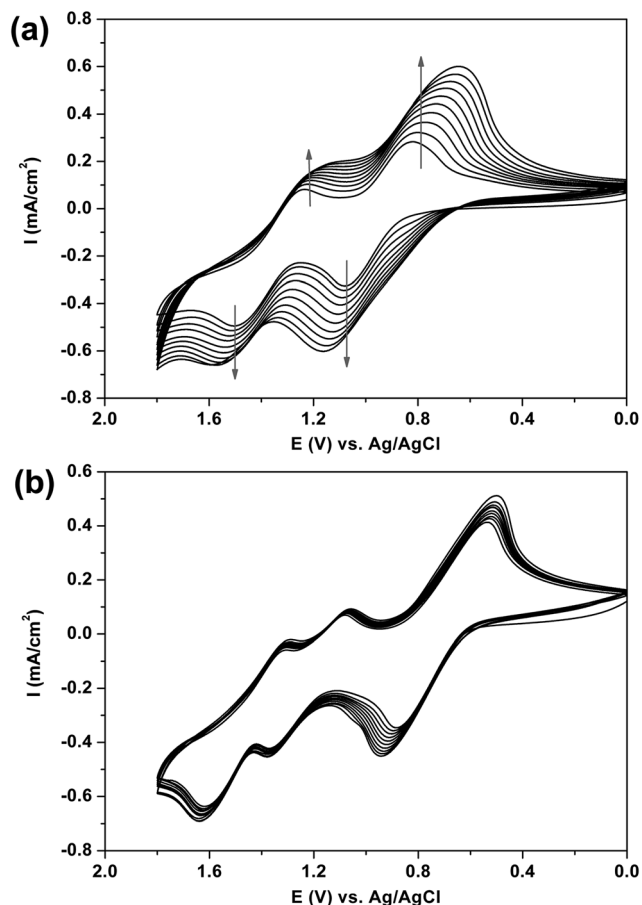


Fig. 2 CV diagrams of the electrodeposition of (a) TPACz and (b) MeOTPACz on ITO-glass, using  $1.0 \times 10^{-3}$  M monomer solutions in 0.1 M TBAP/ACN solution at  $150 \text{ mV s}^{-1}$  during 10 cycles.

$E_{pc} = 0.84$  and  $1.23$  V, which correspond to reduction of film deposited in the preceding anodic scan. In the second and subsequent voltammetric cycles, the anodic peaks gradually shifted to higher potentials and the cathodic peaks shifted to lower potentials with the increasing intensity of the peaks. At the end of CV scan, a visible polymer film was robustly deposited on the working electrode surface. After being immersed in water for a certain period of time, a free-standing polymer film could be detached from the ITO-glass surface. The electrodeposited film of monomer TPACz (coded with PTPACz) is proposed to possess a crosslinked polymer structure formed by the possible TPA-TPA, carbazole-carbazole, and TPA-carbazole coupling reactions. The electrochemical property of MeOTPACz is completely different [Fig. 2(b)]. It is possible to identify three anodic peaks at  $E_{pa} = 0.88$ ,  $1.35$  and  $1.63$  V and three cathodic peaks at  $E_{pc} = 0.55$ ,  $1.07$  and  $1.27$  V in the first CV scan. As the CV scan continued, no significant increase in intensity of these peaks was observed and no polymer film grew up on the electrode surface. The first oxidation process of MeOTPACz occurred at a lower applied voltage than that of TPACz because of the electron-donating methoxy groups substituted at the 4,4'-positions of the TPA unit. The subsequent second and third anodic peaks indicate that the carbazole radical cations were

involved in very fast electrochemical reactions that produced an MeOTPACz dimer  $[(\text{MeOTPACz})_2]$  via the ring-ring coupling reaction between the carbazole units (Scheme 2). The dimer seemed to be the major product during the oxidation process of MeOTPACz, due to the high stability of the oxidized states (bicarbazylum cations).

### Optical and electrochemical properties

Because the polymer film of PTPACz prepared by the electrochemical polymerization is insoluble in organic solvents, we prepared some of the PTPACz sample via the chemical oxidative polymerization of PTPACz using  $\text{FeCl}_3$  in nitrobenzene (see ESI†). Fig. S6† shows the absorption and emission profiles of the monomers and polymers, together with their PL images on exposure to an UV light in both solution and solid states. The relevant absorption and PL data are collected in Table 1. These compounds and their derived polymers exhibited strong UV-vis absorption bands at  $289$ – $347$  nm in  $\text{CH}_2\text{Cl}_2$  solutions, assignable to the  $\pi$ - $\pi^*$  and  $n$ - $\pi^*$  transitions of the carbazole and triphenylamine moieties in the monomer or polymer backbone. The solid state emission spectrum was similar to that recorded from the  $\text{CH}_2\text{Cl}_2$  solution. Although the solid-state emission of PTPACz was found to be slightly red shifted (*ca.*  $13$  nm) from that in solution, the emission remained in the blue region. This polymer in dilute  $\text{CH}_2\text{Cl}_2$  solution exhibited a maximum blue PL emission at  $417$  nm with PL quantum yield of  $28.7\%$ . The red-shift of PL maxima of polymer PTPACz means an extended conjugation length in comparison with the monomer TPACz.

The UV-vis absorption spectra of monomers TPACz and polymer PTPACz both in  $\text{CH}_2\text{Cl}_2$  and the polymer films PTPACz in solid state on an ITO electrode are shown in Fig. S7.† The UV-vis spectrum of TPACz exhibits two main absorption peaks at about  $294$  and  $305$  nm. Due to having extended  $\pi$  conjugation over the polymer backbone, a new broad band was observed at about  $347$  nm in the polymer. The red-shift and broadening of the absorption profile of the polymer film could be attributed to the aggregation of the polymer chains, resulting in a different energy level distribution and enhanced interchain  $\pi$ - $\pi$  interactions in the solid state. The optical band gap values of PTPACz calculated from maximum absorption band edge of solid state was found to be  $2.81$  eV.

The electrochemical behavior of the electrodeposited polymer and dimer films was investigated by CV in a monomer-free TBAP/ACN solution. The quantitative details are summarized in Table 1. As shown in Fig. 3, the CV diagram of PTPACz reveals two reversible oxidation redox couples at half-wave potentials ( $E_{1/2}$ ) of  $0.88$  V and  $1.47$  V. The first anodic peak has been assigned to the one-electron oxidation of the triphenylamine units into the radical cation. When higher potentials are reached, dicationic forms might be obtained in the polymer. The CV curve of dimer (MeOTPACz) $_2$  is essentially identical to that shown in Fig. 2(b). According to the order of oxidation peaks of polymer PTPACz and dimer (MeOTPACz) $_2$ , we propose a possible sequence of reaction under electrochemical oxidation which is shown in ESI Scheme S1.† The HOMO (highest occupied molecular orbital) energy levels of the investigated

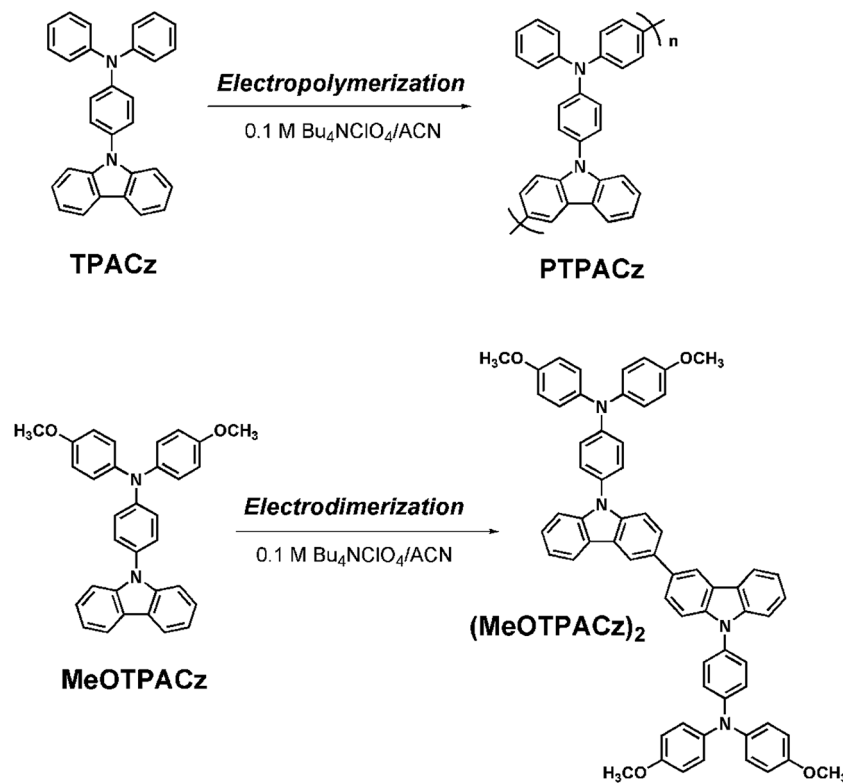
Scheme 2 Synthetic route of polymer PTPACz and dimer (MeOTPACz)<sub>2</sub>.

Table 1 Optical and electrochemical properties of monomers, dimer and polymer

Index	In solution			As solid film <sup>d</sup>			Oxidation potential			Energy levels		
	$\lambda_{\max}^{\text{abs}^a}$ (nm)	$\lambda_{\max}^{\text{PL}^b}$ (nm)	$\Phi_{\text{PL}}^c$ (%)	$\lambda_{\max}^{\text{abs}}$ (nm)	$\lambda_{\text{onset}}^{\text{abs}}$ (nm)	$\lambda_{\max}^{\text{PL}}$ (nm)	$E_{1/2}^{\text{Ox1}}$ (V)	$E_{1/2}^{\text{Ox2}}$ (V)	$E_{1/2}^{\text{Ox3}}$ (V)	$E_g^f$ (eV)	HOMO <sup>g</sup> (eV)	LUMO <sup>h</sup> (eV)
TPACz	294, 305	392	4.5	298, 311	364	—	0.96	1.42	—	3.41	5.31	1.91
PTPACz	294, 347	417	28.7	298, 360	441	424	0.88	1.47	—	2.81	5.24	2.17
MeOTPACz	294	395	3.1	298, 310	375	—	0.71	1.30 <sup>e</sup>	—	3.30	5.07	1.77
(MeOTPACz) <sub>2</sub>	294	408	2.2	298, 310	390	—	0.71	1.20	1.46	3.18	5.07	1.89

<sup>a</sup> Measured in dilute solutions in CH<sub>2</sub>Cl<sub>2</sub> at a concentration of about  $1 \times 10^{-5}$  mol L<sup>-1</sup>. <sup>b</sup> Excited at the absorption maximum. <sup>c</sup> The fluorescent quantum yield was calculated in an integrating sphere with quinine sulfate as the standard ( $\Phi_{\text{PL}} = 54.6\%$ ). <sup>d</sup> Drop-coated from CH<sub>2</sub>Cl<sub>2</sub> solution. <sup>e</sup> Irreversible peak potential ( $E_{\text{pa}}$ ). <sup>f</sup> Optical band gap obtained from  $E_g = 1240/\lambda_{\text{edge}}$ . <sup>g</sup> The HOMO energy levels were calculated from  $E_{1/2}$  and were referenced to ferrocene (4.8 eV). <sup>h</sup> LUMO = HOMO -  $E_g$ .

monomers, dimer and polymer were calculated from the half-wave potentials of the first oxidation wave ( $E_{1/2}^{\text{Ox1}}$ ) and by comparison with ferrocene (4.8 eV). These data together with absorption spectra were then used to obtain the LUMO (lowest unoccupied molecular orbital) energy levels (Table 1).

### Spectroelectrochemical and electrochromic properties

Spectroelectrochemistry were performed on the electro-deposited polymeric and dimeric films on ITO glass to clarify their electronic structures and optical behaviors upon oxidation. The result of polymer PTPACz film is presented in Fig. 4(a) as the UV-vis-NIR absorbance curves correlated to electrode potentials. In the neutral form, at 0 V, PTPACz exhibited strong

absorption at wavelength around 306 nm, characteristic for  $\pi$ - $\pi^*$  transitions, but it was almost transparent in the visible and near infrared (NIR) regions. Upon oxidation of the PTPACz film (increasing applied voltage from 0 to 1.00 V), the absorption peak at 465 nm and a broadband from 800 nm extended to 1100 nm in the NIR region grew up. Since the potentials examined are similar to the first anodic process, the spectral changes are assigned to the radical cation (polaron) formation arising from the oxidation of the TPA unit. The absorption band in the NIR region may be attributed to an intervalence charge transfer (IVCT) between states in which the positive charge is centered at different amino centers (TPA and carbazole). The IVCT phenomenon of the family of triarylamines has been reported

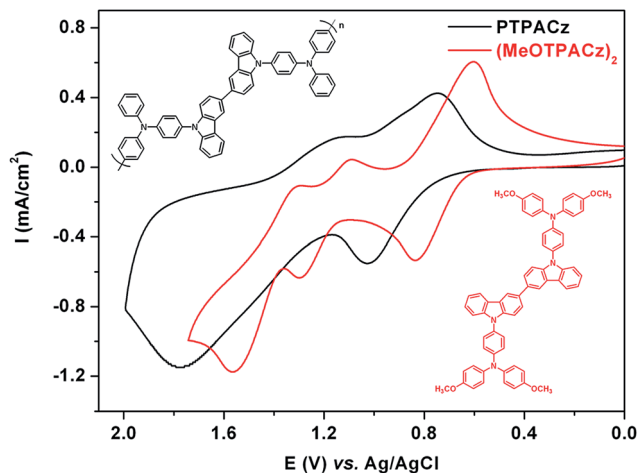


Fig. 3 Cyclic voltammograms of PTPACz and the (MeOTPAcz)<sub>2</sub> dimer in monomer-free 0.1 M TBAP/ACN solution at scan rate 50 mV s<sup>-1</sup>.

in literature.<sup>18,19</sup> Upon further oxidation at applied voltages to 1.8 V, the dication (bipolaron) band at 740 nm formed. Concurrently, the absorption peak at 465 nm decreased in

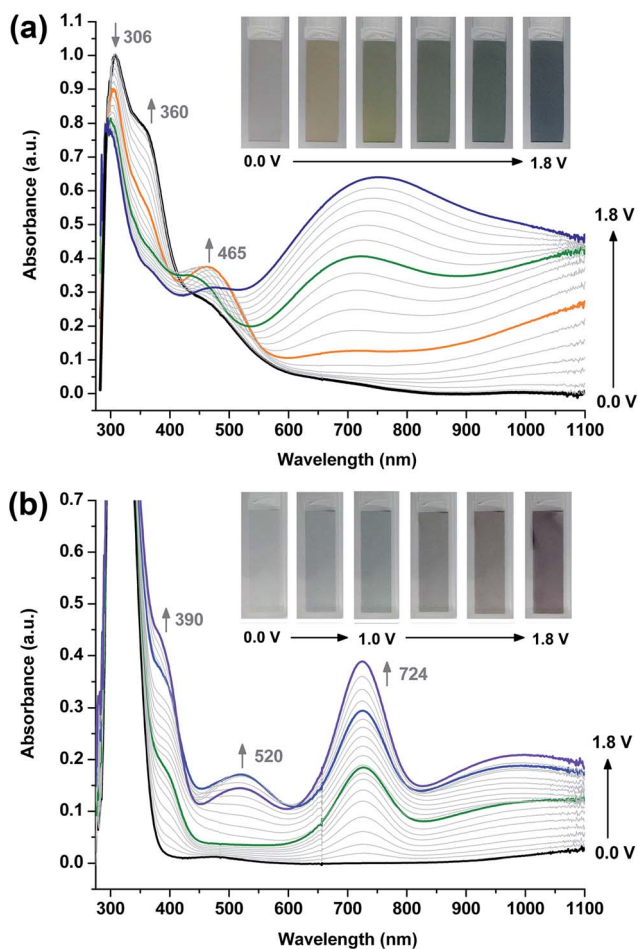


Fig. 4 Spectroelectrograms of (a) PTPACz and (b) (MeOTPAcz)<sub>2</sub> films on ITO-glass substrate in 0.1 M TBAP/ACN solution at applied potentials between 0 and +1.8 V.

intensity during this process. The observed electronic absorption changes in the film of PTPACz at various potentials are fully reversible and are associated with strong color changes; indeed, they even can be seen readily by the naked eye. As shown in Fig. 4(a) inset, it can be seen that the film of PTPACz switches from a transmissive neutral state (nearly colorless) to a highly absorbing semi-oxidized state (pale yellow or yellowish green) and a fully oxidized state (blue). In Fig. 4(b) are depicted the spectral changes of (MeOTPAcz)<sub>2</sub> during the oxidation in 0.1 M TBAP/ACN. The dimeric film showed strong absorption at around 310 nm in the neutral form (0 V). Upon oxidation (increasing applied voltage from 0 to 1.0 V), a new absorption shoulder at 390 and a peak at 724 nm appeared due to the formation of a stable monocation radical of the dimethoxy-substituted TPA unit. Upon further oxidation at applied voltages to 1.8 V, the absorption band at 724 nm increased gradually and a new broad band centered at around 520 nm appeared. The dimer (MeOTPAcz)<sub>2</sub> changed color from a colorless neutral state to light green semi-oxidized states and then to russet at the fully oxidized state.

Electrochromic switching studies for PTPACz were performed to monitor the percent transmittance changes ( $\Delta T$ ) as a function of time at their absorption maximum ( $\lambda_{\text{max}}$ ) and to determine the response time by stepping potential repeatedly between the neutral and oxidized states. The active area of the polymer film on ITO glass is about 1 cm<sup>2</sup>. Fig. 5 depicts the optical transmittance as a function of time at 740 nm by applying square-wave potential steps of 14 s between 0 and 1.4 V for the first 10 cycles. The polymer film still retained reasonable electroactivity after hundreds of cycles. The response time was calculated at 90% of the full-transmittance change because it is difficult to perceive any further color change with naked eye beyond this point. The polymer PTPACz exhibited  $\Delta T$ % up to 68% at 740 nm for blue coloring and required 4.4 s for the

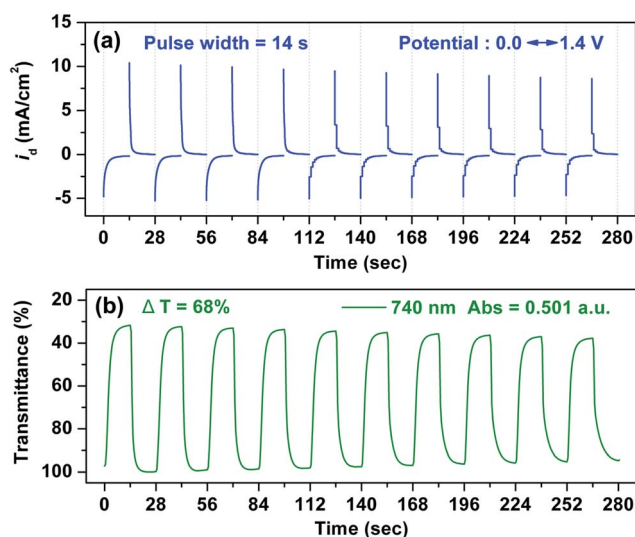


Fig. 5 (a) Electrical current response and (b) transmittance change as a function of time for the deposited film of PTPACz on the ITO-coated glass slide (active area about 1 cm<sup>2</sup>) in 0.1 M TBAP/ACN by applying a potential step between 0.0 and 1.4 V (versus Ag/AgCl).

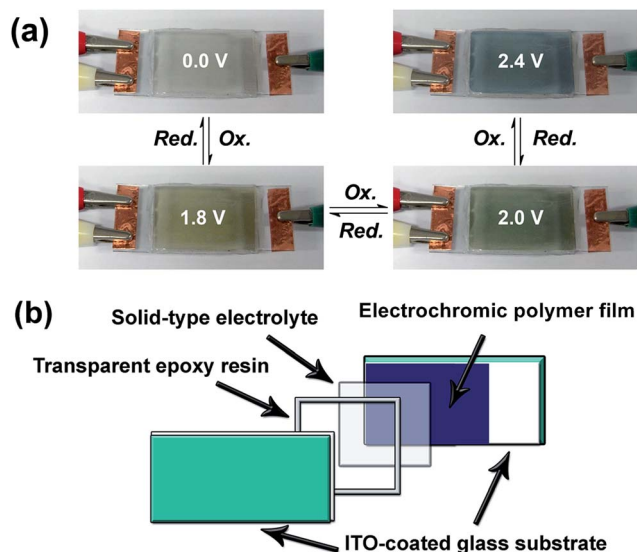


Fig. 6 (a) Pictures of sandwich-type ITO-coated glass electrochromic device, using PTPACz as active layer. (b) Schematic illustration of the assembled ECD.

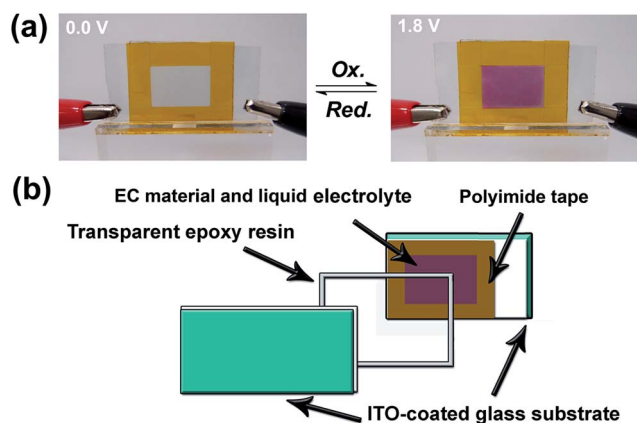


Fig. 7 (a) Photos of sandwich-type ITO-coated glass electrochromic device, using (MeOTPACz)<sub>2</sub> as active layer. (b) Schematic illustration of the assembled ECD.

coloring process and 1.3 s for the bleaching process. The electrochromic coloring efficiency (CE) of blue coloring ( $\eta = \Delta OD_{750}/Q$ ) of the PTPACz film was calculated to be  $158 \text{ cm}^2 \text{ C}^{-1}$ .

### Electrochromic devices

Finally, we fabricated the single layer electrochromic cells as preliminary investigation for their electrochromic applications. The polymeric and dimeric films were electrodeposited onto ITO-coated glass, thoroughly rinsed, and then dried. Afterwards, the gel electrolyte was spread on the polymer-coated side of the electrode and the electrodes were sandwiched. To prevent leakage, an epoxy resin was applied to seal the device. Fig. 6 shows the pictures and schematic illustration of the assembled electrochromic device (ECD) using the PTPACz film as electroactive layer. When the voltage was applied (from 0.0 to 1.8 V, 2.0

V and 2.4 V, respectively), the color changed to yellow, green, and deep blue, respectively, the same as those were already observed in the spectroelectrochemical experiments. The ECD based on dimer (MeOTPACz)<sub>2</sub> was also fabricated as shown in Fig. 7. The device exhibited a russet-pink color while (MeOTPACz)<sub>2</sub> is in the oxidized state. When the potential was subsequently set back at 0.0 V, the polymer and dimer film turned slowly back to original color.

## Conclusions

Two carbazole and triphenylamine-containing monomers TPACz and MeOTPACz were readily synthesized from the Ullmann reaction of *N*-(4-aminophenyl)carbazole with iodobenzene and 4-iodoanisole, respectively. Redox-active and electrochromic polymer film could be robustly deposited on the electrode surface in an electrolyte solution by the electrochemical polymerization of TPACz *via* the arylamine oxidative coupling reactions. However, MeOTPACz formed a dimer film during the CV scanning because the active sites of its TPA unit are blocked with methoxy groups. Both films revealed good electrochemical stability and multi-electrochromic behavior, exhibiting pale yellow, yellowish green, blue, or russet colors, according to their oxidation state. The synthesized TPACz derivatives are promising materials for visible/NIR electrochromic devices because they could be easily prepared from cheap starting materials and could be facily fabricated into electrochromic films *via* electrochemical polymerization.

## Acknowledgements

We thank the Ministry of Science and Technology of Taiwan for financial support of this work.

## References

- (a) P. M. S. Monk, R. J. Mortimer and D. R. Rosseinsky, *Electrochromism: Fundamentals and Applications*, VCH, Weinheim, Germany, 1995; (b) P. M. S. Monk, R. J. Mortimer and D. R. Rosseinsky, *Electrochromism and Electrochromic Devices*, Cambridge University Press, Cambridge, UK, 2007.
- (a) C. G. Granqvist, *Handbook of Inorganic Electrochromic Materials*, Elsevier, Amsterdam, 1995; (b) G. A. Niklasson and C. G. Granqvist, *J. Mater. Chem.*, 2007, **17**, 127–156; (c) D. T. Gillaspie, R. C. Tenent and A. C. Dillion, *J. Mater. Chem.*, 2010, **20**, 9585–9592.
- (a) P. M. S. Monk, *The Viologens: Physicochemical Properties, Synthesis and Applications of the Salts of 4,4'-Bipyridine*, John Wiley and Sons, Chichester, UK, 1998; (b) M. Li, Y. X. Wei, J. M. Zhang, D. Zhu and C. Y. Xu, *Org. Electron.*, 2014, **15**, 428–434.
- (a) S. A. Sapp, G. A. Sotzing, J. L. Reddinger and J. R. Reynolds, *Adv. Mater.*, 1996, **8**, 808–811; (b) A. Kumar, D. M. Welsh, M. C. Morvant, F. Piroux, K. A. Abboud and J. R. Reynolds, *Chem. Mater.*, 1998, **10**, 896–902; (c) L. B. Groenendaal, G. Zotti, P.-H. Aubert, S. M. Waybright

- and J. R. Reynolds, *Adv. Mater.*, 2003, **15**, 855–879; (d) R. M. Walczak and J. R. Reynolds, *Adv. Mater.*, 2006, **18**, 1121–1131.
- 5 (a) F. S. Han, M. Higuchi and D. G. Kurth, *J. Am. Chem. Soc.*, 2008, **130**, 2073–2081; (b) A. Maier, A. R. Rabindranath and B. Tieke, *Adv. Mater.*, 2009, **21**, 959–963; (c) C.-J. Yao, Y.-W. Zhong and J.-N. Yao, *Inorg. Chem.*, 2013, **52**, 10000–10008.
- 6 (a) P. M. Beaujuge and J. R. Reynolds, *Chem. Rev.*, 2010, **110**, 268–320; (b) C. M. Amb, A. L. Dyer and J. R. Reynolds, *Chem. Mater.*, 2011, **23**, 397–415; (c) A. L. Dyer, E. J. Thompson and J. R. Reynolds, *ACS Appl. Mater. Interfaces*, 2011, **3**, 1787–1795; (d) G. Gunbas and L. Toppare, *Chem. Commun.*, 2012, **48**, 1083–1101; (e) L. Beverina, G. A. Pagani and M. Sassi, *Chem. Commun.*, 2014, **50**, 5413–5430.
- 7 (a) P. M. Beaujuge, S. Ellinger and J. R. Reynolds, *Nat. Mater.*, 2008, **7**, 795–799; (b) C. Ma, M. R. Taya and C. Y. Xu, *Polym. Eng. Sci.*, 2008, **48**, 2224–2228; (c) R. Baetens, B. P. Jelle and A. Gustavsen, *Sol. Energy Mater. Sol. Cells*, 2010, **94**, 87–105; (d) G. Sonmez and H. B. Sonmez, *J. Mater. Chem.*, 2006, **16**, 2473–2477; (e) Y. Kondo, H. Tanabe, H. Kudo, K. Nakano and T. Otake, *Materials*, 2011, **4**, 2171–2182; (f) S. Beaupre, A. C. Breton, J. Dumas and M. Leclerc, *Chem. Mater.*, 2009, **21**, 1504–1513; (g) H. T. Yu, S. Shao, L. J. Yan, H. Meng, Y. W. He, C. Yao, P. P. Xu, X. T. Zhang, W. P. Hu and W. Huang, *J. Mater. Chem. C*, 2016, **4**, 2269–2273.
- 8 A. P. Weidner, U.S. Pat., 7450294, 2008.
- 9 M. Thelakkat, *Macromol. Mater. Eng.*, 2002, **287**, 442–461.
- 10 (a) Y. Shirota, *J. Mater. Chem.*, 2000, **10**, 1–25; (b) Y. Shirota, *J. Mater. Chem.*, 2005, **15**, 75–93; (c) Y. Shirota and H. Kageyama, *Chem. Rev.*, 2007, **107**, 953–1010.
- 11 J. V. Grazulevicius, P. Stroehriegl, J. Pielichowski and K. Pielichowski, *Prog. Polym. Sci.*, 2003, **28**, 1297–1353.
- 12 (a) J.-F. Morin, M. Leclerc, D. Ades and A. Siove, *Macromol. Rapid Commun.*, 2005, **26**, 761–778; (b) N. Blouin and M. Leclerc, *Acc. Chem. Res.*, 2008, **41**, 1110–1119; (c) P.-L. T. Boudreault, S. Beaupre and M. Leclerc, *Polym. Chem.*, 2010, **1**, 127–136.
- 13 (a) W.-Y. Lee, T. Kurosawa, S.-T. Lin, T. Higashihara, M. Ueda and W.-C. Chen, *Chem. Mater.*, 2011, **23**, 4487–4497; (b) A.-D. Yu, T. Kurosawa, Y.-C. Lai, T. Higashihara, M. Ueda, C.-L. Liu and W.-C. Chen, *J. Mater. Chem.*, 2012, **22**, 20754–20763; (c) A.-D. Yu, T. Kurosawa, M. Ueda and W.-C. Chen, *J. Polym. Sci., Part A: Polym. Chem.*, 2014, **52**, 139–147.
- 14 (a) M.-Y. Chou, M.-K. Leung, Y.-L. O. Su, C.-L. Chiang, C.-C. Lin, J.-H. Liu, C.-K. Kuo and C.-Y. Mou, *Chem. Mater.*, 2004, **16**, 654–661; (b) H.-J. Niu, H.-Q. Kang, J.-W. Cai, C. Wang, X.-D. Bai and W. Wang, *Polym. Chem.*, 2011, **2**, 2804–2817; (c) L.-N. Ma, H.-J. Niu, J.-W. Cai, P. Zhao, C. Wang, Y.-F. Lian, X.-D. Bai and W. Wang, *J. Mater. Chem. C*, 2014, **2**, 2272–2282; (d) J.-H. Wu and G.-S. Liou, *Adv. Funct. Mater.*, 2014, **24**, 6422–6429.
- 15 (a) S.-H. Cheng, S.-H. Hsiao, T.-H. Su and G.-S. Liou, *Macromolecules*, 2005, **38**, 307–316; (b) G.-S. Liou, S.-H. Hsiao and H.-W. Chen, *J. Mater. Chem.*, 2006, **16**, 1831–1842; (c) C.-W. Chang, G.-S. Liou and S.-H. Hsiao, *J. Mater. Chem.*, 2007, **17**, 1007–1015; (d) H.-J. Yen and G.-S. Liou, *Chem. Mater.*, 2009, **21**, 4062–4070; (e) L.-T. Huang, H.-J. Yen and G.-S. Liou, *Macromolecules*, 2011, **44**, 9595–9610.
- 16 (a) C.-J. Chen, H.-J. Yen, W.-C. Chen and G.-S. Liou, *J. Mater. Chem.*, 2012, **22**, 14085–14093; (b) C.-J. Chen, Y.-C. Hu and G.-S. Liou, *Polym. Chem.*, 2013, **4**, 4162–4171; (c) H.-J. Yen, C.-J. Chen and G.-S. Liou, *Adv. Funct. Mater.*, 2013, **23**, 5307–5316; (d) H.-J. Yen, J.-H. Wu and G.-S. Liou, High Performance Polyimides for Resistive Switching Memory Devices, in *Electrical Memory Materials and Devices*, RSC Polymer Chemistry Series, 2015, ch. 4, pp. 136–166.
- 17 (a) H.-M. Wang and S.-H. Hsiao, *J. Polym. Sci., Part A: Polym. Chem.*, 2014, **52**, 272–286; (b) S.-H. Hsiao, H.-M. Wang and S.-H. Liao, *Polym. Chem.*, 2014, **5**, 2473–2483; (c) H.-M. Wang and S.-H. Hsiao, *J. Mater. Chem. C*, 2014, **2**, 1553–1564; (d) H.-M. Wang and S.-H. Hsiao, *J. Polym. Sci., Part A: Polym. Chem.*, 2014, **52**, 1172–1184.
- 18 M. B. Robin and P. Day, *Adv. Inorg. Radiochem.*, 1967, **10**, 247–422.
- 19 (a) C. Lambert and G. Noll, *J. Am. Chem. Soc.*, 1999, **121**, 8434–8442; (b) A. V. Azeghalmi, M. Erdmann, V. Kriegisch, G. Noll, R. Stahl, C. Lambert, D. Leusser, D. Stalke, M. Zabel and J. Popp, *J. Am. Chem. Soc.*, 2004, **126**, 7834–7845.
- 20 (a) E. T. Seo, R. F. Nelson, J. M. Fritsch, L. S. Marcoux, D. W. Leedy and R. N. Adams, *J. Am. Chem. Soc.*, 1966, **88**, 3498–3503; (b) R. F. Nelson and R. N. Adams, *J. Am. Chem. Soc.*, 1968, **90**, 3925–3930; (c) S. C. Creason, J. Wheeler and R. F. Nelson, *J. Org. Chem.*, 1972, **37**, 4440–4446.
- 21 (a) J. F. Ambrose and R. F. Nelson, *J. Electrochem. Soc.*, 1968, **115**, 1159–1164; (b) J. F. Ambrose, L. L. Carpenter and R. F. Nelson, *J. Electrochem. Soc.*, 1975, **122**, 876–894.
- 22 (a) L. Otero, L. Sereno, F. Fungo, Y.-L. Liao, C.-Y. Lin and K.-T. Wong, *Chem. Mater.*, 2006, **18**, 3495–3502; (b) J. Natera, L. Otero, L. Sereno, F. Fungo, N.-S. Wang, Y.-M. Tsai, T.-Y. Hwu and K.-T. Wong, *Macromolecules*, 2007, **40**, 4456–4463; (c) J. Natera, L. Otero, F. D'Eramo, L. Sereno, F. Fungo, N.-S. Wang, Y.-M. Tsai and K.-T. Wong, *Macromolecules*, 2009, **42**, 626–635; (d) M. I. Mangione, R. A. Spanevello, A. Rumbero, D. Heredia, G. Marzari, L. Fernandez, L. Otero and F. Fungo, *Macromolecules*, 2013, **46**, 4754–4763; (e) S. Koyuncu, B. Gultekin, C. Zafer, H. Bilgili, M. Can, S. Demic, I. Kaya and S. Icli, *Electrochim. Acta*, 2009, **54**, 5694–5702; (f) F. Baycan Koyuncu, *Electrochim. Acta*, 2012, **68**, 184–191; (g) C. Xu, J. Zhao, M. Wang, Z. Wang, C. Cui, Y. Kong and X. Zhang, *Electrochim. Acta*, 2012, **75**, 28–34; (h) S.-H. Hsiao and J.-W. Lin, *Macromol. Chem. Phys.*, 2014, **215**, 1525–1532; (i) S.-H. Hsiao and J.-W. Lin, *Polym. Chem.*, 2014, **5**, 6770–6778.
- 23 (a) C. M. Amb, P. M. Beaujuge and J. R. Reynolds, *Adv. Mater.*, 2010, **22**, 724–728; (b) A. L. Dyer, E. J. Thompson and J. R. Reynolds, *ACS Appl. Mater. Interfaces*, 2011, **3**, 1787–1795; (c) G. Hizalan, A. Balan, D. Baran and L. Toppare, *J. Mater. Chem.*, 2011, **21**, 180–1809; (d) H.-J. Yen and G.-S. Liou, *Polym. Chem.*, 2012, **3**, 255–264; (e) S.-H. Hsiao, H.-M. Wang, P.-C. Chang, Y.-R. Kung and T.-M. Lee, *J.*

- Polym. Sci., Part A: Polym. Chem.*, 2013, **51**, 2925–2938; (f) H.-M. Wang and S.-H. Hsiao, *J. Polym. Sci., Part A: Polym. Chem.*, 2014, **52**, 272–286.
- 24 (a) S. Koyuncu, O. Usluer, M. Can, S. Demic, S. Icli and N. S. Sariciftci, *J. Mater. Chem.*, 2011, **21**, 2684–2693; (b) M. Icli-Ozkut, Z. Oztas, F. Algi and A. Cihaner, *Org. Electron.*, 2011, **12**, 1505–1511; (c) G. Gunbas and L. Toppare, *Chem. Commun.*, 2012, **48**, 1083–1101; (d) E. Karabiyik, E. Sefer, F. Baycan Koyuncu, M. Tonga, E. Ozdemir and S. Koyuncu, *Macromolecules*, 2014, **47**, 8578–8584; (e) B. Karabay, L. C. Pekel and A. Cihaner, *Macromolecules*, 2015, **48**, 1352–1357.